Study of Core Coupling in ^{87}Rb Through Isobaric-Analog Resonances. II*

C. L. Hollas,† H. R. Hiddleston,‡ V. D. Mistry,§ S. Sen, and P. J. Riley
University of Texas, Austin, Texas 78712
(Received 31 January 1972)

The level structure of the ^{86}Kr-^{87}Kr system has been investigated by means of the inelastic scattering of protons through isobaric-analog resonances (IAR's). 24 levels in ^{86}Kr between 1.55 and 5.07 MeV have been identified in the spectra. Excitation-function data indicate that coupling of the $d_{5/2}$ single particle to excited states of ^{86}Kr provides important contributions to the wave function of the IAR's. The coefficients describing the coupling of single-particle states to the excited core states in ^{86}Kr were extracted from the angular-distribution measurements of the inelastic proton decay of the 5.348-, 6.826-, and 8.374-MeV IAR's. The inclusion of these coefficents together with previously deduced elastic spectroscopic factors allows a rather full description of the wave functions for the parent analog states of these IAR's. A calculation of the wave functions and binding energies in terms of a simple core-coupling model has been performed for the d and s states in ^{87}Kr. The calculation shows good agreement with the results of the analysis of the proton decay of the IAR for the low-lying states.

I. INTRODUCTION

In this paper, paper II, we describe the inelastic scattering of protons through IAR in ^{87}Rb, and obtain information on the wave functions of parent analog states in the nucleus ^{87}Kr, as well as on excited states in ^{86}Kr. In paper I, we expressed the parent analog states in ^{87}Kr in the form

$$|\Psi\rangle_J = b_{0J}|\Phi_0 \otimes \Psi_J\rangle_J + \sum_{Ij}{}' b_{Ij}|\Phi_J \otimes \Psi_J\rangle_J ,$$

and reported the determination of the $(b_{0J})^2$ coefficients, which are related to the elastic proton partial widths. In paper II we specifically report on the qualitative and quantitative study of the $(b_{Ij})^2$ coefficients, which are related to the inelastic proton partial widths. In Sec. I of this paper we describe our experimental results, which consist of both proton inelastic excitation function and angular-distribution measurements. We then describe the theoretical analysis used in the extraction of the $(b_{Ij})^2$ coefficients. In Sec. IV we discuss in some detail our data and their analysis at individual resonances. Finally, in Sec. V, we calculate wave functions and binding energies in terms of a simple particle-core coupling model for the d and s states in ^{87}Kr, and compare the calculations with our experimentally deduced results.

II. EXPERIMENTAL RESULTS

The experimental procedure has been described in the previous paper (paper I). A typical pulse-height spectrum, measured at a center-of-mass energy of 9.63 MeV, is shown in Fig. 1. Some contamination, caused by carbon and oxygen, present as carbon dioxide, and by nitrogen, was found to build up slowly within the gas cell during the course of the experiment. The peaks caused by these contaminants are identified in the figure, together with the observed excited states in ^{86}Kr. The over-all experimental resolution was approximately 35 keV. The inelastic data consist of excitation-function measurements at laboratory angles of 95, 125, 145, and 165° in the energy range from 4.76 to 10.10 MeV. Angular distributions were measured at nine IAR's for proton decay to inelastic channels.

A. Determination of Excitation Energy of States in ^{86}Kr

The excitation energies for 24 excited states in ^{86}Kr were determined from proton inelastic scattering at 9.63 MeV. At this energy, many highly excited states (above 3.5 MeV) were observed to resonate with considerable strength. The excita-

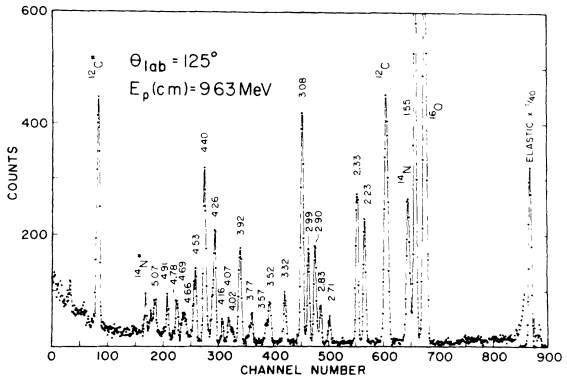

FIG. 1. ^{86}Kr$(p,p')^{86}$Kr pulse-height spectrum taken at a center-of-mass proton energy of 9.63 MeV. The excitation energies of the observed states in ^{86}Kr are indicated in the figure.

tion energies of all the observed inelastic proton groups were obtained by means of a least-squares-fitting code, using the peak locations of (1) ^{86}Kr, ^{16}O, ^{14}N, and ^{12}C elastic states, and (2) the ^{12}C first excited state. Corrections were applied for loss of energy of the reaction particles in passing through the exit gas and Mylar walls using the tables of Williamson and Boujot.[1] A quadratic fit was employed to compensate for the nonlinearity of the energy loss and possible nonlinearity introduced by the electronics. The procedure was repeated for 21 laboratory angles. The results were checked for self-consistency and then averaged. The resulting energy level diagram for ^{86}Kr is shown in Fig. 2. The spin assignments indicated are from a previous analysis of the inelastic scattering of 14.82-MeV protons from ^{86}Kr.[2] The excitation energies are assigned a maximum absolute uncertainty of ±15 keV.

B. Excitation Functions

The inelastic scattering excitation function data are displayed in Figs. 3–5. In general, the data exhibit sharp resonant structure of a simple Breit-Wigner shape, resting on a rather small, flat background.

The excitation functions for the single-phonon $2_1^{(+)}$ and $3_1^{(-)}$ collective-state channels are displayed in Fig. 3. The data for the 2_1^+ channel are composed of two sections, 165° being the observation angle for the data below 7.3 MeV, and 95° for the data above 7.3 MeV. The contaminant lines interfered with the 165° data in the higher-energy region. For both channels the excitation function is dominated by one prominent resonance, the 6.826-MeV IAR for the $2_1^{(+)}$ channel, and the 8.374-MeV IAR for the $3_1^{(-)}$ channel. The $2_1^{(+)}$ channel exhibits a smaller resonance at nearly every elastic resonance energy, which is indicated by the arrows along the bottom of the figure. The $3^{(-)}$ channel does not appear in the data before 7.5 MeV. It resonates weakly at the small negative-parity $l=5$ resonance, as well as at several of the even-parity IAR's.

The 2.23-MeV channel, shown in Fig. 4, exhibits only four resonances over the range of the data, each in conjunction with an even-parity IAR. The high spin of this state (4^+) apparently inhibits its participation in the compound-nuclear wave function. In contrast, the 2.33-MeV channel, with spin 2^+, has an extremely complex resonant behavior. It first appears as a small resonance at the 6.826-MeV IAR (not included in the figure), then resonates at nearly every other IAR, with structure continuing to 10 MeV. The 2.71-MeV channel is essentially inactive, with only one resonance at the $l=2$, 7.463-MeV IAR. The three channels at 2.83, 2.90, and 2.99 MeV exhibit a similar resonant behavior, each obtaining its largest resonance at the $l=2$, 8.142-MeV IAR.

Except for the 3.76-MeV channel, which is essentially inactive, each of the remaining channels shown in Fig. 5 is characterized by a single dominant resonance, which occurs at an energy near the sum of the ground-state, $d_{5/2}$ IAR energy and the excitation energy of the channel. For 12 of the 16 channels this characteristic is observed. Only the 2.23- and 2.33-MeV channels, among those which exhibit appreciable resonant structure, and the weakly excited 2.71- and 3.76-MeV channels

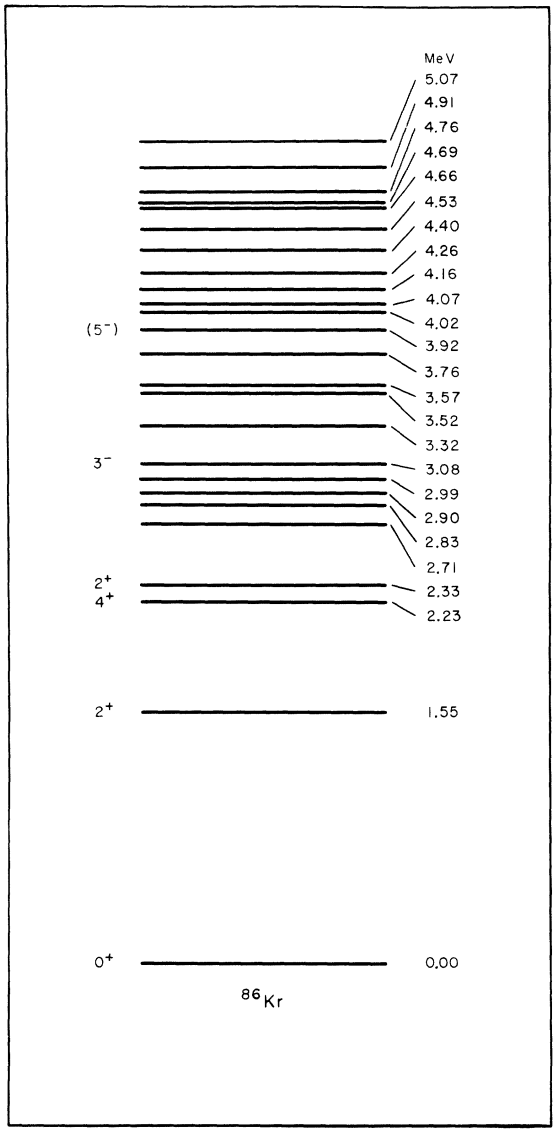

FIG. 2. An energy level diagram for states of ^{86}Kr. The spin assignments are from the work of Ref. 2.

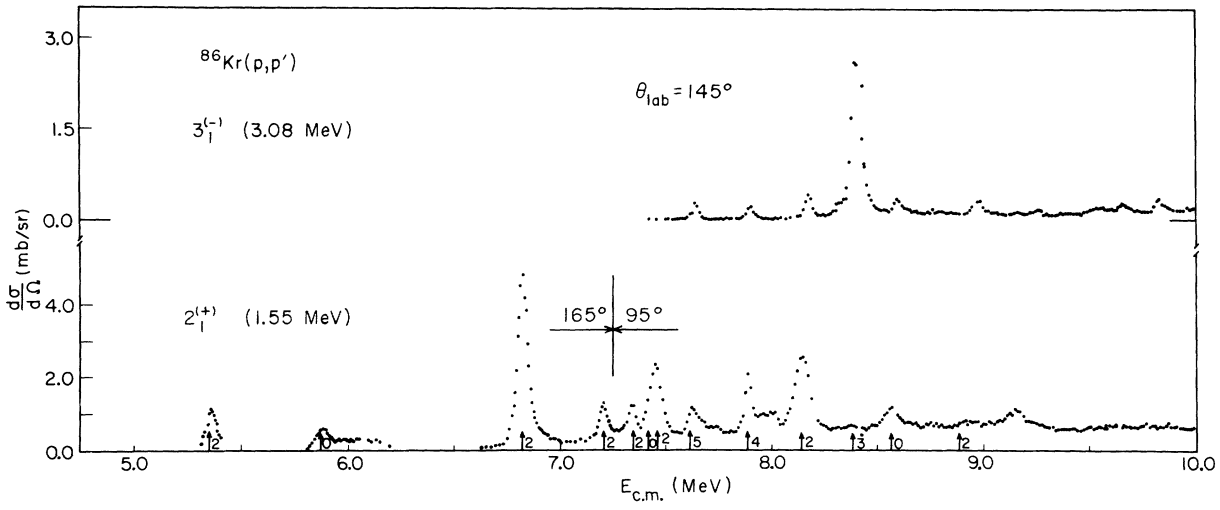

FIG. 3. Inelastic excitation functions for the scattering of protons from the 1.55- and 3.08-MeV states in ^{86}Kr.

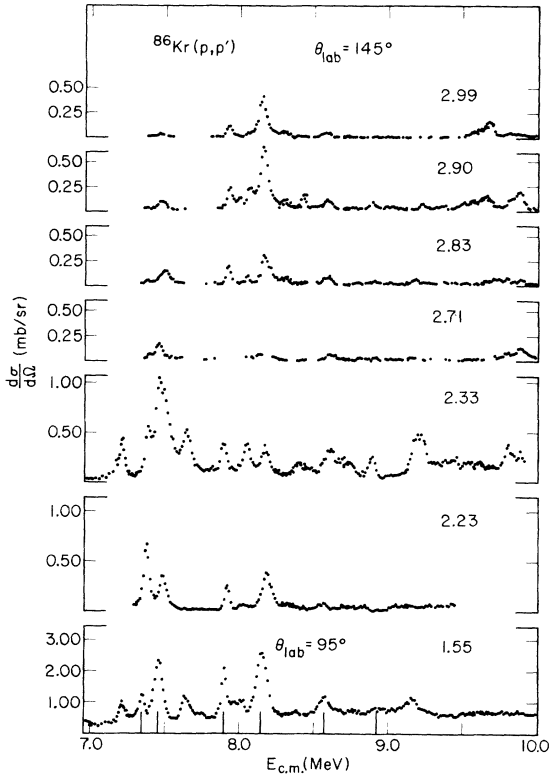

FIG. 4. Inelastic excitation functions for the scattering of protons from ^{86}Kr. All data, except for scattering to the 1.55-MeV state, were taken at a laboratory angle of 145°. Excitation energies of the residual states in ^{86}Kr are indicated in MeV.

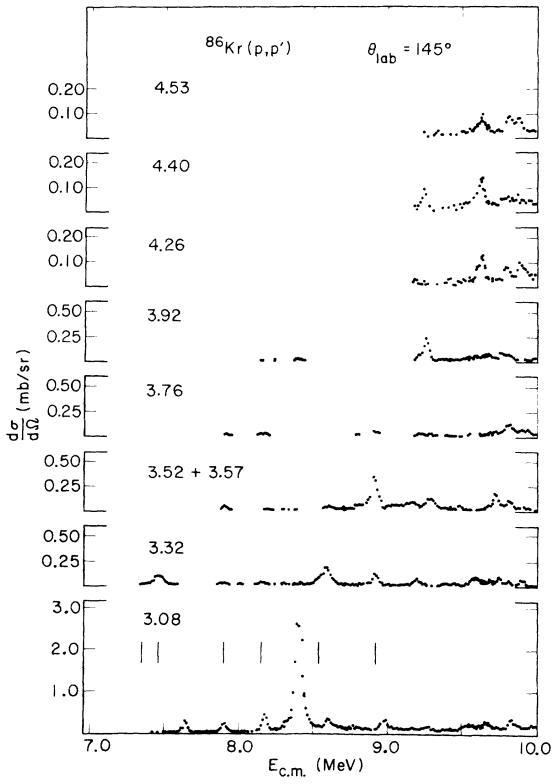

FIG. 5. Inelastic excitation functions for the scattering of protons from ^{86}Kr at a laboratory angle of 145°. Excitation energies of the residual states in ^{86}Kr are indicated in MeV.

do not follow this tendency. Table I summarizes the tendency by listing the energy at which each channel exhibits its largest resonance, in comparison with the excitation energy of the channel plus 5.348 MeV. Such behavior is indicative of the coupling of the $d_{5/2}$ single particle to the excited ^{86}Kr core states.

C. Angular Distributions

Angular distributions were measured at the nine IAR's listed in Table II and are shown in Figs. 6–9. The solid lines are Legendre-polynomial fits to the data; the corresponding Legendre coefficients are listed in Table II. The angular distributions are reasonably symmetric about 90°, indicating that the compound-nuclear-reaction mechanism is dominant. Except for the measurements at the 5.348- and the 7.892-MeV IAR's, the angular distributions for a particular inelastic channel were measured at the energy at which it resonated most strongly. No measurements were made at the 7.420- and 7.463-MeV IAR where the $4_2^{(+)}$ and $2_2^{(+)}$ channels resonate most strongly. These resonances occur in a region where there are three closely spaced IAR's, and the contributions overlap.

III. METHOD OF ANALYSIS

The inelastic spectroscopic factors, $S_{pp'}(Ilj) = (b_{Ij})^2$, for the coupling of the single-particle states to the excited core states are related to the inelastic proton partial widths ($\tilde{\Gamma}_{lj}^{sp'}$) in the same manner as the elastic spectroscopic factors for the coupling of the single-particle states to the ground state are related to the elastic proton decay width, i.e.,[3]

$$\tilde{\Gamma}_{lj}^{sp'} = S_{pp'}\Gamma'_{sp}|a_{\lambda\lambda'}|^{-2}. \quad (1)$$

The single-particle inelastic widths Γ'_{sp} were approximated by the same procedure as the elastic single-particle widths. Each width was determined by calculating the Lane-model elastic proton partial width of the isobaric analog of a single-neutron state of spin j_i and orbital angular momentum l_i lying below the observed analog state at the observed energy of the proton leading to the inelastic channel.[3] The values for $|a_{\lambda\lambda'}|^2$ were taken from the elastic IAR analysis. Thus the inelastic spectroscopic factors were calculated from the ratio

$$S_{pp'}(Ilj) = \tilde{\Gamma}_{lj}^{sp'}|a_{\lambda\lambda'}|^2/\Gamma_{lj}^{sp'}, \quad (2)$$

with

$$\Gamma_{lj}^{sp'} \cong \Gamma'_{sp} = \frac{k'T_0}{E'}\left|\langle\chi_{p'\epsilon}^{(+)}|V_1|\Psi_{nA}\rangle\right|^2. \quad (3)$$

TABLE I. A comparison between the energy, indicated by the third column, at which the strongest resonance is observed in a particular ^{86}Kr$(p,p')^{86}$Kr channel, and the sum of the excitation energy of that channel and 5.35 MeV. This sum is given in the second column.

E^* (MeV)	$E^*+5.35$ (MeV)	E_R MAX (MeV)
1.55	6.90	6.83
2.23	7.58	7.42
2.33	7.68	7.42
2.71	8.12	7.46
2.83	8.18	8.14
2.90	8.25	8.14
2.99	8.34	8.14
3.08	8.43	8.37
3.32	8.67	8.57
3.52	8.87	8.91
3.57	8.92	8.91
3.76	9.11	
3.92	9.27	9.25
4.26	9.61	9.63
4.40	9.75	9.63
4.53	9.88	9.63

TABLE II. Legendre coefficients A_0, A_2/A_0, and A_4/A_0 for the fits to the ^{86}Kr$(p,p')^{86}$Kr inelastic proton angular-distribution data shown in Figs. 6–9. The fits are the solid lines shown in the figures.

E_R (MeV)	J^π	E^* (MeV)	I^π	A_0	A_2/A_0	A_4/A_0
5.348	$\frac{5}{2}^+$	1.55	2^+	−0.0825	0.3709	0.0099
6.826	$\frac{5}{2}^+$, $\frac{3}{2}^+$	1.55	2^+	−0.3696	−0.3517	−0.0086
		2.33	2^+	−0.0126	−0.2555	
7.892	$\frac{7}{2}^+$	2.83		−0.0105	−0.6764	0.0682
		2.90		0.0177	−0.4791	0.0774
		2.99		−0.0045	−0.5941	0.0010
8.142	$\frac{3}{2}^+$	2.83		0.0132	0.7123	−0.1978
		2.90		−0.0290	0.0218	−0.1224
		2.99		0.0391	0.2550	
8.374	$\frac{7}{2}^-$	3.08	3^-	0.1928	0.2904	−0.0425
8.573	$\frac{1}{2}^+$	3.31		0.1849		
8.893	$\frac{3}{2}^+$	3.52				
		3.57		0.2708	0.0815	
9.250		3.92		0.0179	0.0183	0.0099
9.630		3.92		0.0112	0.6060	
		4.26		0.0119	0.5195	
		4.40		−0.0149	0.2598	
		4.53		−0.0092	0.2597	

To extract the inelastic partial widths, the on-resonance angular distributions were fitted using the following expression for the differential cross section[4]:

$$\sigma(\theta)=\frac{(-1)^I\lambda^2\bar{\Gamma}_{lj}}{2[4(E-E_R)^2+I^2]}(2J_0+1)\cos^2\beta\sum_{L=0}^{2J_0+1}P_L(\cos\theta)\bar{Z}(l_0J_0l_0J_0;\tfrac{1}{2}L)$$

$$\times\sum_{j_1j_2}(-1)^{j_1+j_2}\cos(\delta_{j_1}-\delta_{j_2})(\pm)(\bar{\Gamma}^{sp'}_{l_1j_1})^{1/2}(\pm)(\bar{\Gamma}^{sp'}_{l_2j_2})^{1/2}\bar{Z}(l_1j_1l_2j_2;\tfrac{1}{2}L)W(j_1J_0j_2J_0;IL)\,. \quad (4)$$

This expression describes the decay of a compound-nuclear resonance of spin J_0 and orbital angular momentum l_0 to the residual nuclear state of spin I by emission of protons of spin j_i and orbital angular momentum l_i. $\bar{\Gamma}_{lj}$, Γ, and E_R are the elastic proton partial width, total width, and resonance energy. The δ_{ij} are optical-model phase shifts calculated at the energy of the outgoing proton. The $(\pm)(\bar{\Gamma}^{sp'}_{ij})^{1/2}$ are the inelastic proton partial-width amplitudes and are the only free parameters in the equation. The derivation of the above expression assumes that no direct processes are involved, and that the Hauser-Feshbach compound-nuclear contributions are negligible. The data indicate that these conditions are fulfilled rather well, as the resonance to off-resonance ratios for the observed cross sections are greater than 10 to 1, with essentially flat off-resonance backgrounds in the excitation functions, and the angular distributions show rather strong symmetry about 90°.

IV. RESULTS AND DISCUSSION

The cross-section expression given above was programmed into the computer code BACCHUS-APOLLO[5] and was used to fit the inelastic angular-distribution data by variation of the partial widths. The extraction of these widths were prejudiced in the sense that the largest value for the $d_{5/2}$ partial width was sought, since the energy for the $d_{5/2}$ single-particle wave function lies nearest to the correct energy to couple with the core excitation to provide the total excitation energy of the compound system. It was necessary to include some $s_{1/2}$ admixture in all cases.

A. 5.348-MeV IAR

The 5.348-MeV resonance was identified in paper I as the IAR of the $d_{5/2}$ ground state of ^{87}Kr, with an elastic spectroscopic factor of 0.62. The only inelastic transition observed at this energy is a resonance in the 1.55-MeV (2^+) channel. The on-resonance angular distribution of protons to this channel and the fit generated with Eq. (4) are presented in Fig. 6. The wave function for this IAR is dominated by the $d_{5/2}$ single-particle wave function coupled to the 0^+ ground state of ^{86}Kr. The next largest contribution, 11%, arises from coupling the $d_{5/2}$ single particle to the 1.55-MeV (2^+) excited core state. Coupling of the $s_{1/2}$ single-particle state to the 2^+ core also provides a small contribution.

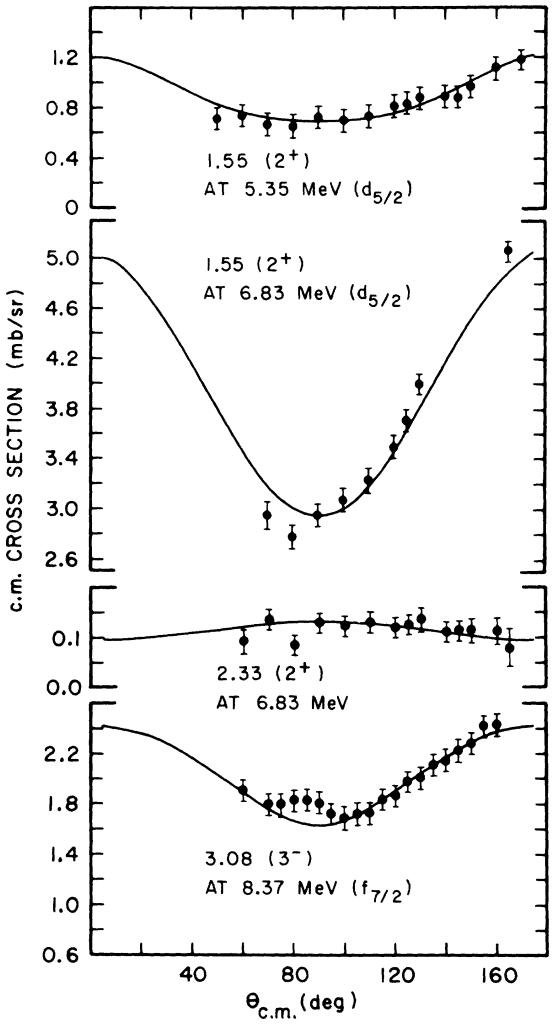

FIG. 6. Inelastic angular distributions for the scattering of protons from ^{86}Kr at IAR's in ^{87}Rb. The excitation energies of the residual states in ^{86}Kr and the energies of the IAR's at which the data were measured are indicated in the figure.

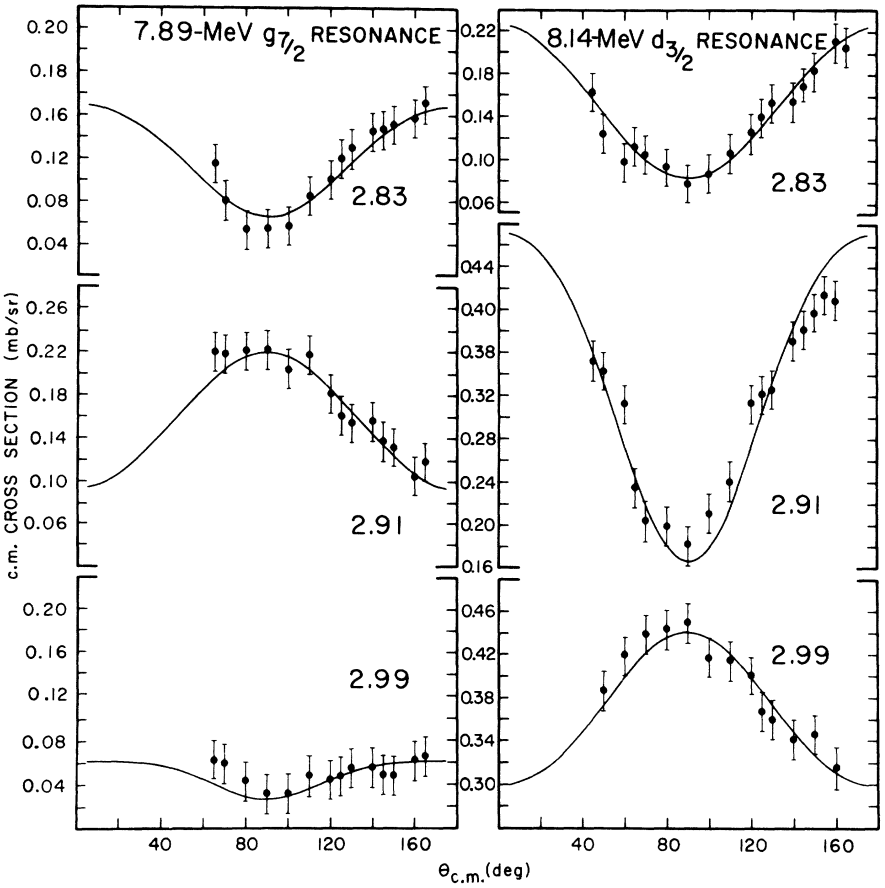

FIG. 7. Inelastic angular distributions for the scattering of protons from ^{86}Kr at the 7.89- and 8.14-MeV IAR's in ^{87}Rb. The excitation energies of the residual states in ^{86}Kr are indicated in MeV.

B. 6.826-MeV IAR

The 6.826-MeV resonance was identified in paper I as the IAR of the second $l=2$ state of ^{87}Kr, at an excitation energy of 1.468 MeV, with possible spin assignments of $d_{5/2}$ or $d_{3/2}$. The 1.55-MeV channel displays a very prominent resonance at this IAR, as seen in Fig. 3. The energy of 6.826 MeV, which is 1.478 MeV above the ground-state $d_{5/2}$ IAR, is favorable for the coupling of the $d_{5/2}$ single particle to the 1.55-MeV state. The only other inelastic channel with any activity is the 2.33-MeV channel, which exhibits a small resonance.

The on-resonance angular distributions of the inelastic protons to these two channels and the fits generated with Eq. (4) are presented in Fig. 6. Equally good fits were obtained under both the $d_{5/2}$ and the $d_{3/2}$ spin assumptions for the IAR. For the spin value $\frac{5}{2}^+$ the large $d_{5/2}$ inelastic partial width indicates that the wave function for this IAR has a large component composed of the $d_{5/2}$ single-particle state coupled to the 1.55-MeV excited core state, and actually the wave function appears to be dominated by this configuration. In addition there is a significant contribution arising from the $s_{1/2}$ single-particle state coupled to this excited core state, with minor contributions involving the 2.33-MeV excited core state.

C. 8.374-MeV IAR

The 8.374-MeV IAR was identified in paper I to be an odd-parity, $l=3$ IAR and was assigned a spin of $\frac{7}{2}^-$. This is the first $l=3$ resonance to appear in the data, and falls below the expected centroid energies of both the $f_{7/2}$ and $f_{5/2}$ orbits. The elastic analysis indicated a small spectroscopic factor for the coupling of the single-particle state to the 0^+ ground state. As was the case for the 6.826-MeV IAR, the energy is favorable for the coupling of the $d_{5/2}$ state to the 3.08-MeV excited core state. The 3.08-MeV channel resonates strongly at this energy, and since the 3.08-MeV

state carries spin and parity of 3^-, vector coupling with the $d_{5/2}$ state to a compound state of spin $f_{7/2}$ is easily attained.

The on-resonance angular distribution of the inelastic protons to this channel is presented in Fig. 6 along with the fit generated with Eq. (4). The analysis indicates that the IAR is dominated by coupling to the 3.08-MeV excited core state, with the coupling to the $d_{5/2}$ single-particle state being the most important, but also with significant coupling to the $s_{1/2}$ single-particle state. The wave function for the parent analog state in ^{87}Kr then has the form

$$|\Psi_{7/2}\rangle = \pm(0.03)^{1/2}\,|\Phi_0 \otimes f_{7/2}\rangle \pm (0.31)^{1/2}\,|\Phi_3 \otimes d_{5/2}\rangle_{7/2} \pm (0.21)^{1/2}\,|\Phi_3 \otimes s_{1/2}\rangle_{7/2} + \cdots .$$

The sum over the $(b_{Ij})^2$ coefficients totals 0.54, in contrast to nearly unity for the 6.826-MeV IAR. The parent state in ^{87}Kr is highly excited at 3.028 MeV, but this is still somewhat low for the energy expected for the $f_{7/2}$ single-particle state, which lies across the energy gap in the next major neutron shell. Apparently, only a small fraction of the $f_{7/2}$ strength is mixed into this state, which has the major portion of its wave function made up from even-parity single-particle states coupled to the 3^- excited core state. Single-particle widths, experimental partial widths, and coupling coefficients derived from the fits to the inelastic angular distributions at the 5.348-, 6.926-, and 8.374-MeV resonances are listed in Table III.

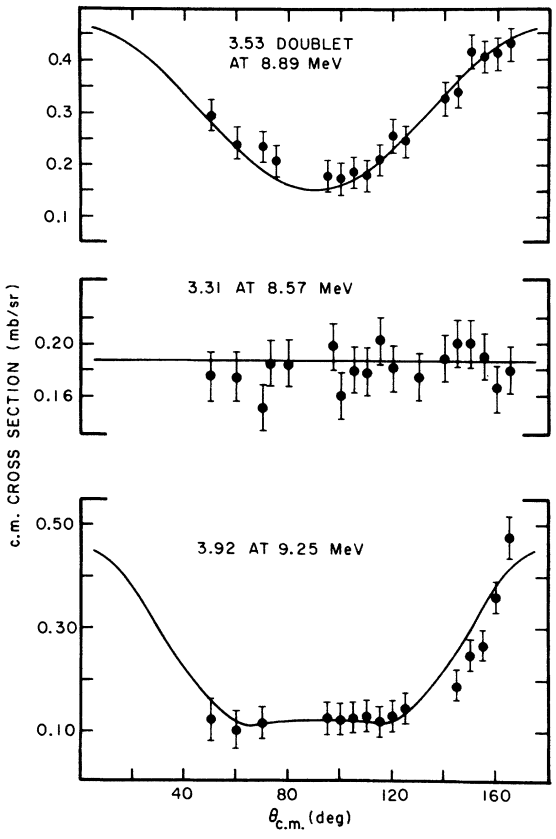

FIG. 8. Inelastic angular distributions for the scattering of protons from ^{86}Kr at IAR's in ^{87}Rb. The excitation energies of the residual states in ^{86}Kr and the energies of the IAR's at which the data were measured are indicated.

D. 9.63-MeV IAR

The 9.63-MeV IAR could not be analyzed to extract the l value, partial width, and total width. However, some features about this resonance should be discussed. In the inelastic excitation function data, Fig. 5, a group of states above 4 MeV is observed to resonate at 9.63 MeV. In fact, at this energy many states of excitation energy in the neighborhood of 4.5 MeV are seen for the first time in the data.

The expected excitation energy centroid for $[d_{5/2} \otimes g_{9/2}^{-1}]_{J\pi}$ neutron particle-hole excitations from the $N = 50$ closed shell is near 4.5 MeV. In ^{88}Sr, Cosman and Slater,[6] using the reaction ^{87}Sr-$(d, p)^{88}$Sr, observed six rather strong transitions

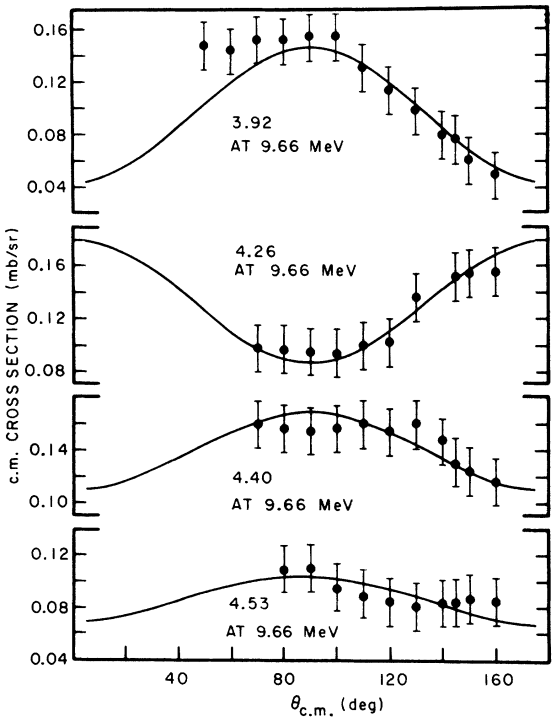

FIG. 9. Inelastic angular distributions for the scattering of protons from ^{86}Kr at the 9.63-MeV IAR in ^{87}Rb. The excitation energies of the residual states in ^{86}Kr are indicated.

TABLE III. Single-particle widths, $\Gamma_J^{sp'}$, experimental partial widths, $\tilde{\Gamma}_J^{sp}$, and core coupling coefficients $(b_{Ij})^2$ deduced from the analysis of the ^{86}Kr$(p,p')^{86}$Kr data at the 5.348-, 6.826-, and 8.374-MeV IAR's, respectively.

E_R (MeV)	J^π	E^* (MeV)	I^π	$\Gamma_{5/2}^{sp'}$ (keV)	$\Gamma_{1/2}^{sp'}$ (keV)	$\Gamma_{3/2}^{sp'}$ (keV)	$\tilde{\Gamma}_{5/2}^{sp'}$ (keV)	$\tilde{\Gamma}_{1/2}^{sp'}$ (keV)	$\tilde{\Gamma}_{3/2}^{sp'}$ (keV)	$(b_{0J})^2$	$(b_{I,5/2})^2$	$(b_{I,1/2})^2$	$(b_{I,3/2})^2$	$\sum(b_{I,f})^2$
5.348	$\frac{5}{2}^+$	1.55	2_1^+	2.0	32.5		0.22	0.92	0.10	0.62	0.11	0.03		0.75
6.826	$\frac{5}{2}^+$	1.55	2_1^+	10.0	54.0	14.0	6.1	9.4	0.7	0.18	0.61	0.18	0.05	
		2.33	2_2^+	2.7	44.0		0.45	0.08			0.02	<0.001		1.04
	$\frac{3}{2}^+$	1.55	2_1^+	10.0	54.0		5.3	8.9		0.22	0.54	0.17		
		2.33	2_2^+	2.7	44.0		0.45	0.02			0.02	<0.001		0.95
8.374	$\frac{7}{2}^-$	3.08	3_1^-	10.0	54.0		2.3	11.0		0.03	0.31	0.21		0.54

to states centered about 4.57 MeV, which probably have this particle-hole configuration. Ball and Fulmer[7] investigated states of this nature in ^{90}Zr with the reaction ^{91}Zr$(p,d)^{90}$Zr, and also observed six rather strong transitions to states centered about 4.79 MeV. It is thus reasonable to assume that the states in ^{86}Kr near 4.5 MeV in excitation energy that resonate at 9.63 MeV are members of the $[2^+, 3^+, 4^+, 5^+, 6^+, 7^+]$ multiplet possible from the angular momentum coupling of a $d_{5/2}$ neutron to a $g_{9/2}$ neutron hole.

As the results for the 6.826-MeV and the 8.374-MeV IAR indicate, when an IAR occurs at an energy which is near the sum of the ground-state $d_{5/2}$ IAR plus the excitation energy of a state in ^{86}Kr, it is possible for the wave function for that IAR to be dominated by the coupling of a $d_{5/2}$ single particle to the excited ^{86}Kr core state. Thus the IAR at 9.63 MeV could have, as a major configuration, a $d_{5/2}$ single-particle state coupled to the excited core states which have an excitation energy near $9.63 - 5.38 = 4.28$ MeV.

Assuming that the states in ^{86}Kr near 4.28 MeV which resonate at 9.63 MeV are the $[d_{5/2} \otimes g_{9/2}^{-1}]_{J^\pi}$ neutron particle-hole excitations, and that the IAR has as a component of its wave function a $d_{5/2}$ particle coupled to the excited core state, this component of the IAR wave function would then consist of two particles in the $d_{5/2}$ orbit, and one hole in the $g_{9/2}$ orbit. The simplest structure would have the two $d_{5/2}$ particles coupled to zero angular momentum, with the angular momentum of the IAR provided by the $g_{9/2}$ hole.

The angular distributions for the inelastic proton decay to the four strongest states, namely those at 3.92, 4.26, 4.40, and 4.53 MeV, were calculated under the above assumption using Eq. (4). Only the decay of a $d_{5/2}$ particle was considered. The final state spins in ^{86}Kr were searched to reproduce the shape of the angular distributions, and the magnitude of the cross-section data reproduced by adjusting the size of the $d_{5/2}$ inelastic partial width. To obtain the calculated cross sections shown in Fig. 9, the following spin assignments were required: 3.92 MeV (5^+), 4.26 MeV (7^+), 4.40 MeV (4^+), 4.53 MeV (4^+). Since the magnitude of the elastic proton partial width was not available, only relative magnitudes for the $d_{5/2}$ inelastic widths are extracted, and are listed in Table IV.

Under the above assumptions, the parent analog wave function the 9.63-MeV IAR would have

TABLE IV. Excitation energies, possible spin assignments, and relative $d_{5/2}$ partial widths for the ^{86}Kr states observed to resonate at the 9.63-MeV IAR. These states are assumed to have a neutron particle-hole character.

E^* (MeV)	I^π	$\tilde{\Gamma}_{I,5/2}$
3.92	5^+	0.75
4.26	7^+	0.79
4.40	4^+	1.00
4.53	4^+	0.61

TABLE V. A comparison of experimental and calculated centroid binding energies of neutron single-particle states in ^{87}Kr.

J^π	$\bar{E}_{Bn}$ (exp) (MeV)	$\bar{E}_{Bn}$ (cal) (MeV)
$\frac{5}{2}^+$	5.005	5.266
$\frac{1}{2}^+$	4.329	3.955
$\frac{3}{2}^+$	3.058	3.205
$\frac{7}{2}^+$	2.997	4.077

the structure:

$$|\Psi\rangle_{9/2} = N\{(b_{0,9/2})|\Phi_0 \otimes g_{9/2}\rangle_{9/2} \pm (0.75)^{1/2}|[d_{5/2}\otimes g_{9/2}^{-1}]_{5^+}\otimes d_{5/2}\rangle_{9/2} \pm (0.79)^{1/2}|[d_{5/2}\otimes g_{9/2}^{-1}]_{7^+}\otimes d_{5/2}\rangle_{7/2}$$
$$\pm (1.00)^{1/2}|[d_{5/2}\otimes g_{9/2}^{-1}]_{4^+}\otimes d_{5/2}\rangle_{9/2} \pm (0.61)^{1/2}|[d_{5/2}\otimes g_{9/2}^{-1}]_{4^+}\otimes d_{5/2}\rangle_{9/2} + \cdots\}.$$

Entrance to the IAR would be necessary through the $|\Phi_0 \otimes g_{9/2}\rangle$ configuration. The elastic excitation function data would reveal the presence of this term by an $l=4$ resonance at 9.63 MeV. The data, shown in paper I, do show some structure at this energy, but the characteristic $l=4$ shape is not discernible in this region. However, by 9.63 MeV, the density of states is becoming rather high, and the individual resonances are overlapping. Ball and Fulmer[7] have investigated parent analog states of the two-particle–one-hole configuration with the neutron pickup reaction ^{92}Zr-$(p,d)^{91}$Zr, where the neutron is taken from the $g_{9/2}$ orbit. It is certainly possible that a two-particle–one-hole state is seen here as an IAR, with the $d_{5/2}$ proton decay to the $[d_{5/2}\otimes g_{9/2}]_{J^\pi}$ neutron particle-hole excited states of ^{86}Kr. Similar IAR's have not previously been reported in this or any other mass region.

Much of the above is speculation. However, the ability to reproduce the angular distributions with the assumptions made, and using only the single inelastic decay width is surprising.

V. CALCULATION OF NEUTRON STATES IN ^{87}Kr

The experimental study of the elastic and inelastic proton decay of the IAR indicates that the coupling of single-particle states to the excited states of ^{86}Kr provides a significant contribution to the wave functions of states in ^{87}Kr. It was of interest, therefore, to attempt a calculation for the states of ^{87}Kr in terms of a core-coupling model.

A. Coupled Equations

The Schrödinger equation for the ^{87}Kr system is

$$H\Psi = E\Psi\ , \tag{5}$$

where the Hamiltonian H is assumed to have the form

$$H = T + H_t + V_{\mathrm{DIAG}} + V_{\mathrm{COUPL}}\ . \tag{6}$$

T is the kinetic energy operator for the neutron, H_t is the Hamiltonian for the ^{86}Kr system, V_{DIAG} is a real Woods-Saxon optical-model potential for the extra neutron, and V_{COUPL} is the interaction

TABLE VI. A comparison of the experimental and calculated binding energies and core-coupling coefficients for $\frac{5}{2}^+$, $\frac{3}{2}^+$, and $\frac{1}{2}^+$ states in the ^{87}Kr system.

E^* (MeV)	E_B (exp) (MeV)	$(b_{0J})^2$	$(b_{2,5/2})^2$	$(b_{2,1/2})^2$	E_B(cal) (MeV)	$(b_{0J}^{\mathrm{cal}})^2$	$(b_{2,9/2}^{\mathrm{cal}})^2$	$(b_{2,7/2}^{\mathrm{cal}})^2$	$(b_{2,5/2}^{\mathrm{cal}})^2$	$(b_{2,3/2}^{\mathrm{cal}})^2$	$(b_{2,1/2}^{\mathrm{cal}})^2$
					$J^\pi = \frac{5}{2}^+$						
0.000	5.516	0.62	0.11	0.03	5.340	0.720	0.118	0.005	0.122	0.006	0.029
1.468	4.044	0.18	0.61	0.18	3.461	0.094	0.005	0.006	0.862	0.003	0.030
1.996	3.516	0.10			2.480	0.001		0.923			0.075
					$J^\pi = \frac{1}{2}^+$						
0.529	4.983	0.62			4.903	0.594			0.370	0.036	
2.080	3.432	0.20			3.004	0.295			0.605	0.100	
3.225	2.287	0.11			1.343	0.118			0.019	0.864	
					$J^\pi = \frac{3}{2}^+$						
2.112	3.400	0.50			4.262	0.524		0.130	0.265	0.030	0.051
2.775	2.737	0.10			3.511	0.129		0.097	0.723	0.014	0.037
2.823	2.689	0.11									
3.015	2.497	0.08									
3.545	1.967	0.03			0.241	0.002		0.316		0.001	0.680

potential which provides the coupling of the various single-particle bound states to the core states.

The wave function for the system is assumed to have the form

$$|\Psi\rangle_J = b_{0J}|\Phi_0 \otimes \nu_J\rangle_J + \sum_{Ij}{}' b_{Ij}\,|\Phi_I \otimes \nu_j\rangle_J = \sum_{Ij} b_{Ij}\,|\Phi_I \otimes \nu_j\rangle_J\,, \tag{7}$$

where the sum extends over the states I of the core and the available single-particle states j. The radial portion of the single-particle wave function is separated out such that

$$|\Psi_J\rangle = \frac{1}{r}\sum_{Ijl} b_{Ij}U_{jl}(r)\,|\Psi_{jl} \otimes \Phi_I\rangle_{JM}\,. \tag{8}$$

The Φ_I satisfy the Schrödinger equation for the core system

$$H_t\,\Phi_I = \omega_I\,\Phi_I\,, \tag{9}$$

where ω_I is the excitation energy of the Ith state. The $|\nu_j\rangle$ are the neutron single-particle bound-state wave functions of spin j and satisfy

$$(T + V_{\mathrm{DIAG}})\,|\nu_j\rangle = \overline{E}_B(j)\,|\nu_j\rangle\,. \tag{10}$$

$\overline{E}_B(j)$ is the centroid binding energy for a neutron in the single-particle orbit j bound in the Woods-Saxon well V_{DIAG}.

If we insert Eq. (9) into Eq. (5), we can obtain, after some algebraic manipulation, the following:

$$\left[\frac{d^2}{d\rho^2} - \frac{l(l+1)}{\rho^2} - \frac{V_{\mathrm{DIAG}}}{E_J} + 1\right] b_{Ij}U_{lj}(r) = \frac{1}{E_J}\sum_{I'j'l'} b_{I'j'} \times \langle\langle(\Psi_{jl} \otimes \Phi_I)\,|\,V_{\mathrm{COUPL}}\,|\,\Psi_{j'l'} \otimes \Phi_{I'}\rangle\rangle\, U_{j'l'}(r)\,. \tag{11}$$

The above set of coupled differential equations for the radial bound-state wave functions $U_{jl}(r)$, has been programmed into the code NEPTUNE for numerical solution by Tamura.[8] With a given set of optical-potential parameters, the solution to the equations provides the set of coupling coefficients $(b_{Ij})^2$ associated with a particular value for the energy $E_J = \overline{E}_B(j) - \omega_I$.

B. Coupling to the 0$^+$ Ground State

The calculation was performed first with only the coupling to the ground state of ^{86}Kr considered, i.e. with V_{COUPL} set to zero. This calculation yields the centroids for the binding energies associated with the neutron single-particle states, and the neutron bound-state wave functions. The energies are listed in Table V along with the experimentally determined centroid separation energies $\overline{E}_{Bn}$(EXP), as determined for a particular spin J, from the expression

$$\overline{E}_{Bn}(\mathrm{EXP}) = \sum_i (b_{0J})_i^2 E_{Bn}(J)_i \Big/ \sum_i (b_{0J})_i^2\,, \tag{12}$$

where $(b_{0J})^2$ is the elastic spectroscopic factor determined in paper I from the analysis of the elastic decay of the IAR for the ith resonance of spin J. $E_{Bn}(J)_i$ is the experimental separation energy of the parent of that state.

The bound-state calculations were made using the Woods-Saxon geometric parameters used in the (d, p) analysis of Haravu *et al.*,[9] with a real-well depth of 48.8 MeV and spin-orbit well depth of 6.25 MeV.

The d and s centroids are in fairly good agreement with the experimental values, while the high spin value $g_{7/2}$ appears bound much less strongly than the calculated value. By varying the real well depth it was possible to reproduce precisely the experimental separation energies for each spin value. The final value of the potential depth was selected as an average value from the individual sets available.

C. Coupling to the 0$^+$ Ground State and to the 2$^+$ First Excited State

Using the same optical-potential parameters as in the preceding section, the calculation for the $d_{5/2}$, $s_{1/2}$, and $d_{3/2}$ states were repeated with coupling to the first excited state (2$^+$, 1.55 MeV) of ^{86}Kr included. The coupling strength parameter in V_{COUPL}, $\beta_{02} = 0.11$ was taken from the coupled-channel analysis for the proton inelastic scattering to the 1.55-MeV state.[2]

The single-particle strength for each spin value was split into three levels by the introduction of the coupling interaction. The binding energies and the calculated coefficients $(b_{0J}^{\mathrm{cal}})^2$ and $(b_{Ij}^{\mathrm{cal}})^2$ are listed in Table VI, along with the experimentally determined values. A calculated level was assigned a correspondence to that experimental level having a separation energy and a spectroscopic factor coupling to the ground state nearest to the calculated values. A comparison of the calculated and experimental results is shown in Fig. 10.

1. $d_{5/2}$ States

The calculated $d_{5/2}$ binding energies were, respectively, 5.340, 3.461, and 2.480 MeV. The first value corresponds to the experimentally observed ground state of ^{87}Kr, which has a separation energy of 5.516 MeV. The elastic spectroscopic factor of 0.62 compares favorably with the calculated value of 0.72. The remainder of the wave function for this state is largely accounted for by coupling the $d_{5/2}$ single particle to the 2$^+$

core in both the experimental $[(b_{2,5/2})^2 = 0.13]$ and calculated $[(b^{cal}_{2,5/2})^2 = 0.122]$ results. There are minor contributions resulting from coupling the 2^+ core to the $s_{1/2}$ and $d_{3/2}$ states.

The second calculated level at 3.461 MeV can be associated with the $l = 2$ experimental level at 4.044 MeV if the spin is assumed to be $d_{5/2}$. The elastic spectroscopic factor was found to be 0.18, compared with a calculated value of 0.094. As previously discussed, we believe that the 4.044-MeV state is dominated by a $d_{5/2}$ single particle coupled to the 2^+ core, with the $(b_{2,5/2})^2$ value of 0.61. The calculation supports this contention, as indicated by the large $(b^{cal}_{2,5/2})^2 = 0.862$ value. Both the experimental and calculated results indicate small contributions from the 2^+ core coupling to the $s_{1/2}$ single particle.

The third calculated binding energy of 2.480 MeV cannot be associated with any of the observed levels. The calculation indicates a very small elastic spectroscopic factor, and that the wave function is dominated by the 2^+ core coupled to the $g_{7/2}$ single particle.

2. $s_{1/2}$ States

The calculation yields three $s_{1/2}$ binding energies at 4.903, 3.004, and 1.343 MeV. The lowest level can be associated with the second excited state of ^{87}Kr with a separation energy of 4.983 MeV. The elastic spectroscopic factor $(b_{0,1/2})^2 = 0.62$ is in good agreement with the calculated value of 0.59. No analysis was performed on the inelastic proton decay of this IAR, and thus no $(b_{2j})^2$ values are available for comparison with the calculated values. The calculation indicates that the remainder of the wave function may be considered to be a $d_{5/2}$ neutron coupled to the 2^+ core. In the excitation function measurements, (Fig. 3), a resonance is observed in the 1.55-MeV channel at this IAR.

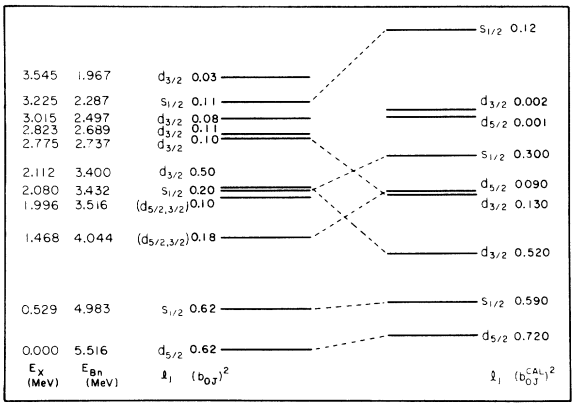

FIG. 10. A comparison between the experimental and calculated $d_{5/2}$, $d_{3/2}$, and $s_{1/2}$ states in ^{87}Kr. The first two columns list the respective experimental excitation energies and separation energies. The calculated binding energies are indicated by the position of the second column of horizontal lines. The correspondence between experimental and calculated states is indicated by the dashed lines.

The binding energy eigenvalue of 3.004 MeV can be associated with the second $s_{1/2}$ state with a separation energy of 3.432 MeV. The elastic spectroscopic factor of 0.20 is comparable to the calculated value of 0.295. The calculation indicates that a large portion, $(b^{cal}_{2,5/2})^2 = 0.605$, of the wave function is found in the $d_{5/2}$ particle coupled to the 2^+ core component. The 1.55-MeV channel does resonate strongly at this energy; however, there are several closely spaced resonances in this energy region, and the effects of the individual resonances are difficult to separate.

The third binding energy eigenvalue of 1.343 MeV can probably be associated with the only other observed $s_{1/2}$ state, with separation energy of 2.287 MeV. The elastic spectroscopic factor for this IAR was determined to be 0.11, while the calculation yields a value of 0.118. The calculation suggests that the remainder of the wave function lies in the $d_{3/2}$ particle coupled to the 2^+ core component.

3. $d_{3/2}$ States

The calculated $d_{3/2}$ binding energies were, respectively, 4.262, 3.511, and 2.411 MeV. The 4.262-MeV level has a calculated $(b^{cal}_{0,3/2})^2$ value of 0.52. Other than the ground state, the only observed $l = 2$ level with a large elastic spectroscopic factor is the state with separation energy of 3.400 MeV and with $(b_{0,3/2})^2 = 0.50$. We therefore believe that we can associate these two states with each other. No experimental $(b_{2j})^2$ coefficients are available for comparison with the calculated values.

The 3.511-MeV state has a calculated elastic spectroscopic factor of 0.129. Of the $l = 2$ states available, there are three candidates for association with this calculated level; the 2.775-MeV level with $(b_{0,3/2})^2 = 0.10$; the 2.823-MeV level with $(b_{0,3/2})^2 = 0.11$; and the 3.015-MeV level with $(b_{0,3/2})^2 = 0.08$.

The third value for the binding energy, 2.411 MeV, has a small, $(b^{cal}_{0,3/2})^2 = 0.002$ value associated with it. Correspondence to any observed level is not possible.

VI. SUMMARY AND COMMENTS

The level structure of ^{86}Kr has been investigated by means of the inelastic scattering of protons.

24 levels between 1.55 and 5.07 MeV have been identified in the spectra.

Excitation function data at IAR's indicate that the coupling of the $d_{5/2}$ single-particle wave function to the excited states of ^{86}Kr provides important contributions to the wave function of the IAR's. For 12 of the 16 inelastic channels at which excitation-function measurements were carried out, the data can be characterized by a single dominant resonance, which occurs at an energy near the sum of the ground-state, $d_{5/2}$ IAR energy and the excitation energy of the channel.

The core-coupling coefficients describing the coupling of the single-particle states to the excited core states in ^{86}Kr were extracted from the angular distribution measurements of the inelastic proton decay of the 5.348-, 6.826-, and 8.374-MeV IAR's. The inclusion of these coefficients together with the previously deduced elastic spectroscopic factors allows a rather full description of the wave function for the parent analog states of these IAR's. The 6.826-MeV IAR wave function is dominated by a configuration consisting of a $d_{5/2}$ particle coupled to the 1.55-MeV core state. The 8.374-MeV IAR wave function is dominated by the coupling of a $d_{5/2}$ single particle to the 3.08-MeV excited core state, with, in addition, significant coupling of an $s_{1/2}$ single particle to the 3.08-MeV state.

A group of states of excitation energy of approximately 4.5 MeV is observed to resonate at the 9.63-MeV IAR. We speculate that the observed inelastic states are members of the $[d_{5/2} \otimes g_{9/2}^{-1}]_{J^\pi}$ neutron particle-hole multiplet, and that consequently the 9.63-MeV IAR is dominated by a $d_{5/2}$ single particle coupled to neutron particle-hole excited core states. Thus, the IAR would essentially consist of a two-particle–one-hole configuration, with subsequent $d_{5/2}$ proton decay.

A calculation of the wave functions and binding energies in terms of a simple core-coupling model has been performed for the d and s states in ^{87}Kr. The calculation shows good agreement with the results from the analysis of the proton decay of the IAR for the low-lying states, but the agreement deteriorates as higher excited levels are considered.

---

*Research supported in part by the U. S. Atomic Energy Commission.

†Present address: Department of Nuclear Physics, The Australian National University, Box 4, P.O., Canberra, A.C.T., Australia.

‡ Present address: Department of Physics, University of Notre Dame, Notre Dame, Indiana 46556.

§ Present address: Radiation Therapy Department, Holy Cross Hospital, Austin, Texas 78702.

[1]C. Williamson and J. P. Boujot, Centre d'Etudes Nucléaires de Saclay Report, 1962 (unpublished).

[2]C. L. Hollas, H. R. Hiddelston, P. J. Riley, and S. Sen, Bull. Am. Phys. Soc. 15, 1682 (1970).

[3]P. A. Moore, P. J. Riley, C. M. Jones, M. D. Mancusi, and J. L. Foster, Jr., Phys. Rev. Letters 22, 356 (1969).

[4]S. A. A. Zaidi and P. Dyer, Phys. Rev. 185, 1332 (1969).

[5]P. A. Moore and H. R. Hiddleston, private communication.

[6]E. R. Cosman and D. C. Slater, Phys. Rev. 172, 1126 (1969).

[7]J. B. Ball and C. B. Fulmer, Phys. Rev. 172, 1199 (1969).

[8]T. Tamura, Center for Nuclear Studies, University of Texas Report, 1971 (unpublished).

[9]K. Haravu, C. L. Hollas, P. J. Riley, and W. R. Coker, Phys. Rev. C 1, 938 (1970).